International Journal of Pharmaceutics 647 (2023) 123518

Contents lists available at ScienceDirect

International Journal of Pharmaceutics

journal homepage: www.elsevier.com/locate/ijpharm

Laser-cutting: A novel alternative approach for point-of-care manufacturing of bespoke tablets

Yujing Liu [a], Anna M Leonova [a], Paul G. Royall [a], Bambang V.E.B. Abdillah Akbar [a], Zhengge Cao [a], Stuart A. Jones [a], Abdullah Isreb [b], Daniel B. Hawcutt [c,d], Mohamed A. Alhnan [a,*]

[a] Centre for Pharmaceutical Medicine Research, Institute of Pharmaceutical Science, King's College London, London, UK
[b] School of Pharmacy and Biomolecular Sciences, Liverpool John Moores University, Liverpool, UK
[c] NIHR Alder Hey Clinical Research Facility, Alder Hey Children's NHS Foundation Trust, Liverpool, UK
[d] Department of Women's and Children's Health, University of Liverpool, Liverpool, UK

ARTICLE INFO

Keywords:
CNC
Early phase clinical trials
Subtractive manufacturing
Patient-specific
Personalized
Small batch

ABSTRACT

A novel subtractive manufacturing method to produce bespoke tablets with immediate and extended drug release is presented. This is the first report on applying fusion laser cutting to produce bespoke furosemide solid dosage forms based on pharmaceutical-grade polymeric carriers. Cylindric tablets of different sizes were produced by controlling the two-dimensional design of circles of the corresponding diameter. Immediate and extended drug release patterns were achieved by modifying the composition of the polymeric matrix. Thermal analysis and XRD indicated that furosemide was present in an amorphous form. The laser-cut tablets demonstrated no significant drug degradation (<2%) nor the formation of impurities were identified. Multi-linear regression was used to quantify the influences of laser-cutting process parameters (laser energy levels, scan speeds, and the number of laser applications) on the depth of the laser cut. The utility of this approach was exemplified by manufacturing tablets of accurate doses of furosemide. Unlike additive or formative manufacturing, the reported approach of subtractive manufacturing avoids the modification of the structure, e.g., the physical form of the drug or matrix density of the tablet during the production process. Hence, fusion laser cutting is less likely to modify critical quality attributes such as release patterns or drug contents. In a point-of-care manufacturing scenario, laser cutting offers a significant advantage of simplifying quality control and a real-time release of laser-cut products such as solid dosage forms and implants.

1. Introduction

Creating personalised medicines, medical devices, and implants necessitates precise, quick, and adaptable qualities and the ability to manufacture customised dosage forms at the point of care (PoC). In the past decade, additive manufacturing technologies such as semi-solid extrusion (Öblom et al., 2019), fused deposition modelling (Krueger et al., 2022; Melnikova et al., 2014; Sadia et al., 2018), powder bed fusion (Awad et al., 2020) and inkjet (Kyobula et al., 2017) 3D printing technologies were also heavily researched to realise the potential of PoC manufacturing. These technologies permit the creation of patient-specific medical devices and dosage forms in small batches at or near medical facilities, such as hospital pharmacies (Trenfield et al., 2018). Nevertheless, 3D printing technologies have several limitations such as low output, thermal post-treatment steps, drug degradation, and a relatively long manufacturing time per tablet (Choonara et al., 2016). In addition, both formative (powder compression or injection moulding) and additive (3D printing) manufacturing approaches induce significant changes to the starting material such as matrix density and the formation of the amorphous form of the drug (Crișan et al., 2022; Kozakiewicz-Latała et al., 2022). Therefore, it is essential to develop process analytical technology tools to monitor the product during and following manufacturing at the point of care (Yang et al., 2023a, b). There are limited examples of using subtractive manufacturing for pharmaceutical applications. For instance, die-cutting involves the removal of excess raw material through complex tooling to produce a product of the desired shape and size (Peng et al., 2017). Recently, computer numerical control (CNC) carving was reported to achieve accurate dosing of

* Corresponding author at: Centre for Pharmaceutical Medicine Research, Institute of Pharmaceutical Science, King's College London, 150 Stamford Street, London SE1 9NH, United Kingdom.
E-mail address: Alhnan@kcl.ac.uk (M.A. Alhnan).

https://doi.org/10.1016/j.ijpharm.2023.123518
Received 13 July 2023; Received in revised form 2 October 2023; Accepted 15 October 2023
Available online 16 October 2023

hydrocortisone tablets from a drug-polymer cast (Kaba et al., 2023). Fig. 1 provides an overview of different established and proposed manufacturing methods of personalised solid dosage forms in the pharmaceutical field.

Laser-cutting technology is a form of subtractive manufacturing that is widely used in the production of biomedical devices built from biodegradable polymers (Albarahmieh et al., 2019; Cairone et al., 2022), with examples including magnesium stents, and intraocular lenses (Heberle et al., 2018). Laser-cutting offers several advantages such as the ability to create small and precise cuts and to minimise dust and waste formation (Caiazzo et al., 2005a). In the process, laser power, cutting speed, nozzle diameter, and focus point position can influence the kerf width and the edge quality of the cut. The process has been used to curve polymethacrylate (Elsheikh et al., 2020) and polycarbonate (Moradi et al., 2021), and to process 3D printed structures (Moradi et al., 2020). Yet, there have been no previous reports on applying laser cutting to produce dosage forms or drug-eluting implants.

Subtractive manufacturing technologies by laser are often referred to as i) flame, ii) fusion or iii) remote (vapour) laser cutting. In flame laser cutting, chemical and physical reactions occur within the material due to the dehydration, carbonization and/or the decomposition of the workpiece e.g., calcium carbonate or wood structure (Guo et al., 2021). In fusion laser cutting (remove), the surface temperature reaches the melting temperature of the workpiece following laser beam application, and the process creates a molten pool in the material removal area (Seo et al., 2020). Then, the material is removed by applying a stream of inert auxiliary gas e.g., N_2. In remote laser cutting, the surface temperature of the workpiece reaches the gasification temperature upon laser application, and the melt pool contents partially evaporate (Seo et al., 2020).

Children undertaking cardiac surgery or suffering from heart failure are prescribed diuretics such as furosemide (Prandota, 2001). The standard furosemide dose for children with normal renal function is 1 to 2 mg/kg. Due to the extended half-life of the medicine in the infant's body, accumulation may occur, and a recognised adverse effect is sensorineural hearing loss (Brion et al., 2001). Moreover, an overdose of furosemide in children may increase other risks including hypovolemia, gallstones, and hypercalciuria (Brion et al., 2001). Therefore, providing children with individualised precise dosing is highly beneficial. Solid dosage forms such as oral tablets and implants are mainly manufactured using a formative manufacturing method such as powder compression in a metal die or injection moulding (Sandler et al., 2011a). These methods for manufacturing solid dosage forms are well-established and economical (Littler and Morrow, 1999). However, the process is geared toward mass production and the process is too rigid and expensive for manufacturing bespoke doses (Khaled et al., 2014).

In this work, we evaluate for the first time using laser cutting as a method for the on-demand manufacturing of oral solid dosage forms, and its potential to overcome some challenges associated with 3D printing and powder compression technologies. To achieve this, specially designed prefabricated drug-polymer castings were used as a substrate (workpiece), to be cut *via* fusion laser cutting process. To maintain low energy input, the surface of the specially designed drug-polymer workpiece absorbs the laser energy and reaches its melting point. Then, the margins removal step was simplified to suit point-of-care manufacturing by replacing the auxiliary gas stream with purpose-built cross-shaped pistons that support the tablets while allowing the passive discharge of the molten mass on the laser path. Furosemide, a molecule liable to light and temperature degradation, was used as a model drug to investigate the impact of laser on drug degradation.

2. Materials and methods

2.1. Materials

Furosemide (>97 %), and polyethene glycol 400 (PEG 400) and 6,000 (PEG 6,000) were purchased from Alfa Assar (Massachusetts, USA). Kolliphor® P188 Geismar was a donation from BASF (Ludwigshafen, Germany). Glyceryl monostearate (GMS) (Imitators K900) was donated by Oleo GmbH (Hamburg Germany). Candurin® Gold sheen, Blue Shimmer and Silver Sheen were provided by Merck (Darmstadt, Germany). All other materials were of a reagent grade.

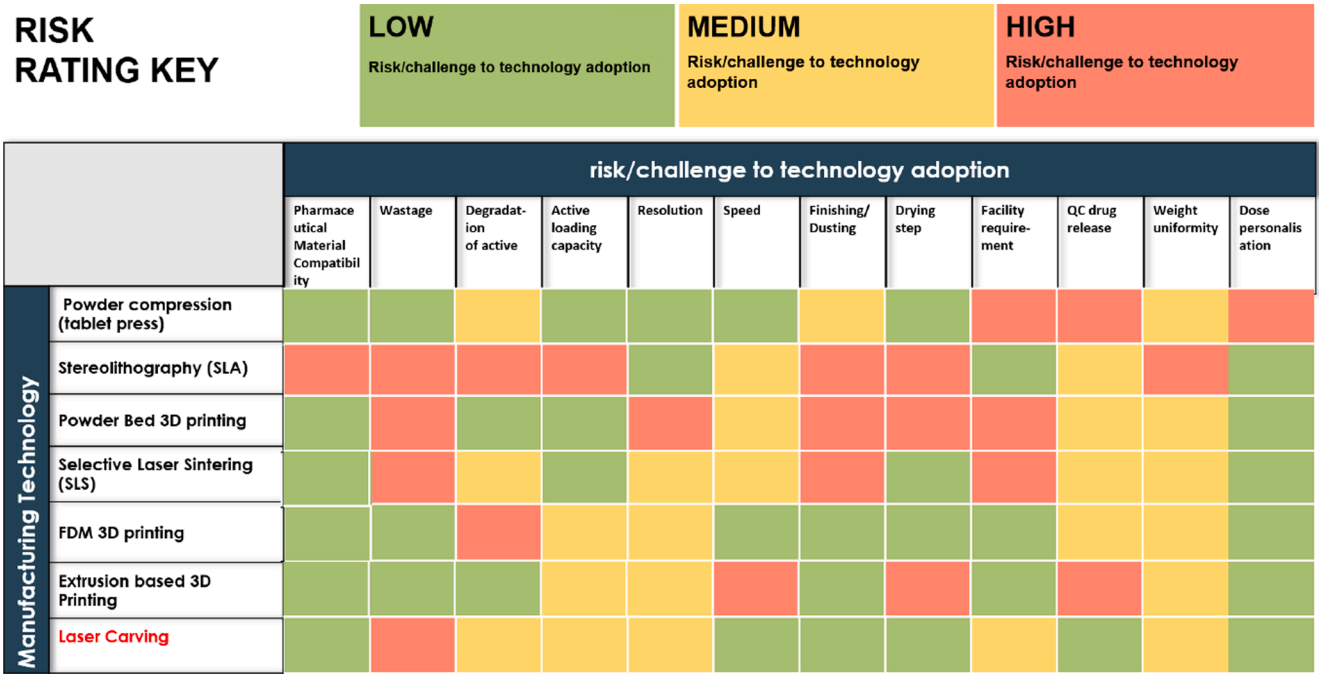

Fig. 1. Overview of different manufacturing methods using established formative manufacturing (powder compression), additive manufacturing (3DP) and the proposed subtractive manufacturing (CNC carving). Laser cutting offers unique features of minimal QC (major implications on batch release following manufacturing) compared to other methods.

2.2. Design of the 3D printing template for drug-polymer casts

The supporting templates (83 × 83 × 8 mm) with 25 cross-shaped support pistons (8 × 8 × 5 mm) were specially designed to accommodate the casting (77 × 77 × 3 mm) template (Supplementary data, Fig. S1). All templates were manufactured using stereolithography 3D printer Form2 (Formlabs, Massachusetts, USA) and a flexible photopolymeric methacrylate resin (Flexible80A).

2.3. Preparation of drug-polymer casts

To facilitate the absorption of laser light by the substrate, different light absorbents, including sodium chloride, Blue Shimmer, Silver Sheen, and Gold Sheen, were added to PEG 6000 at 5 % (w/w). The concentration of the selected light absorbent was optimised using lower concentrations (1 %, 2 % or 3 % w/w), and 1 % w/w of Gold Sheen was used as the optimal light absorbent concentration. Poloxamer K188 and GMS were added as a hydrophilic binder and lubricant to enhance matrix solidification and the ratio in the formulation was set at 7 % and 3 % (Kuźmińska et al., 2021), respectively. Supplementary Data, Table S1 provides a summary of the composition of 6 drug-polymer casts to provide immediate and extended-release formulation. A drug-polymer cast (60 g) with dimensions (length × width × height = 77 × 77 × 3 mm) was prepared as detailed in Fig. 2. Firstly, glass plates and 3D printed templates were placed in an oven at 40 °C to prevent the molten material from rapid cooling. Then, PEG 6000, GMS, and Poloxamer K188 were co-melted and blended at 75 °C using a magnetic stirring hot plate. Furosemide powder was added to the blend under continuous stirring at 75 °C and stirred for an additional 5 min until a clear solution was achieved. Then, Gold Sheen was then added under a consistent stirring to the molten blend prior to casting. Finally, the resultant molten blend was poured into a pre-warmed 3D printed casting template and a glass plate was slowly applied with the 3D printed template to ensure the formation of the flat surface of the drug-polymer cast. Following the cooling of the device to room temperature, the glass plate was removed to yield the workpiece for laser cutting (Supplementary Data Fig. S1).

2.4. Process parameters of the laser cutting process parameters

The prepared drug-polymer casts were directly placed in an Emblazers 2 benchtop laser cutter (Darkly Labs, Melbourne, Australia). To optimise the process of laser cutting, four parameters were assessed: speed, power, counts of laser cutting, as well as margin distance between the tablets. Firstly, the laser power was set at 2.25 Watts for this study to find the ideal laser speed. The cutting speed was adjusted to 10, 50, 100, 200, 500, or 1000 mm/min for one cutting turn. For optimal laser power, the laser power was adjusted to 1.5, 1.75, 2, 2.25, 2.5, 2.75, or 3 Watts, where cutting counts and speed were set at 25 counts and 1000 mm/min, respectively. Thirdly, the number of repeated laser path were optimised by adjusting the number of cutting counts to 1, 5, 10, 20, or 50 counts under constant laser power of 2.25 Watts and a cutting speed of 1000 mm/min. Finally, to determine the optimal margin between the two tablets, the laser power and cutting speed were fixed at 2.25 Watts

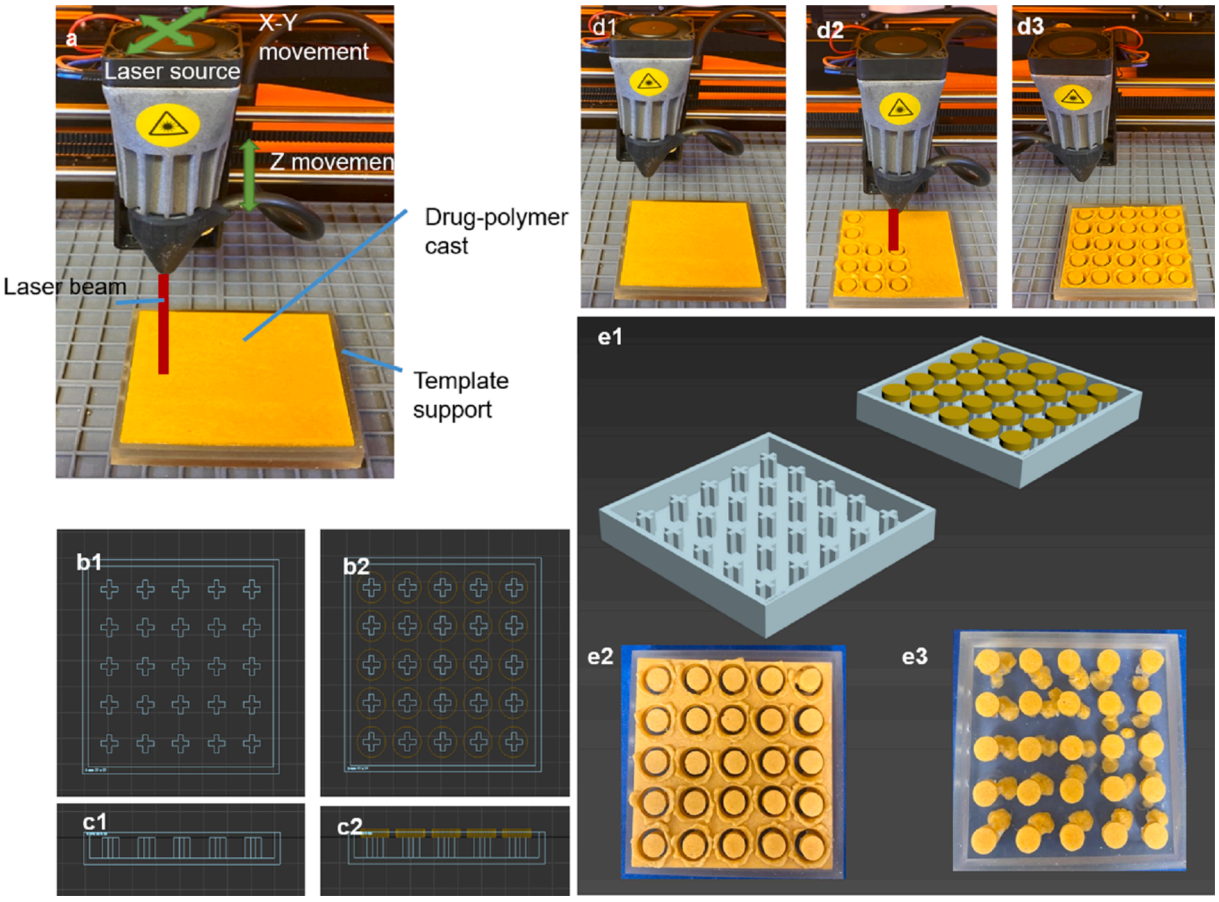

Fig. 2. (**a**) The setup of the laser cutting station: a specially made drug-polymer cast (workpiece) is placed in 3D printed template holder. The setup is enclosed in a confined chamber equipped with high-performance filtration unit. (**b1, b2**) Top and (**c1, c2**) side views of 3D printed template to support the polymerics casts during laser cutting process, each tablet will be supported by a cross-shaped pistol that allows the discharge of the molten casts. Yellow circles show the position of the tablets (**b2, c2**). (**d1-d3**) Steps of laser cutting process of furosemide loaded cast: (**d1**) setting origin (starting point); (**d2**) tablets cutting; (**d3**) the end the of the cutting process. (**e1**) Rendered image of blank support template and following laser cutting. Batch of laser-cut the ablets placed in the supporting template: **e2**) before and **e3**) after removal of out-cut frame. (For interpretation of the references to colour in this figure legend, the reader is referred to the web version of this article.)

and 1000 mm/min, while the distance between the two tablets was adjusted to 0, 1, 2, 3, or 4 mm. To achieve complete separation from the workpiece, a minimal number of counts while maintaining a smooth finishing of the cutting edge, the following laser cutting process parameters were selected: laser energy of 2.25 Watts, laser speed of 1000 mm/min, and cutting times: 25 counts.

2.5. Tablet design and laser cutting

The Lightburn software V1.4.0 (Darkly Labs, Melbourne, Australia) enabled the control of the weight of the tablets by changing the diameter of the laser cutting circle and the production of four tablet batches. The target weight of the tablets could be determined based on the percentage of furosemide loading of the casting, the volume of the cut cylinder, and the target dose of the furosemide. Emblaser 2 benchtop laser cutter (Darkly Labs, Melbourne, Australia) was loaded with furosemide casts, and tablets were cut as specified in Section 2.4 (Fig. 2d1-d3, Supplementary Data, Video S1). A batch of 25 tablets was produced. The diameter of the laser cutting circle was set at 7.6, 8.8, 10, or 11.5 mm to achieve tablets of an approximate diameter of 5, 7.5, 10, or 15 mg, respectively. The engravement on the surface of the tablets was achieved by applying the following settings: 5 counts, laser energy of 2.25 Watts, and a laser speed of 1000 mm/min.

2.6. Thermogravimetric analysis (TGA)

The thermal degradation of the raw materials, physical mixtures, and laser-cut tablets were analysed by scanning samples in platinum pans one run per sample with a TGA Q500 (TA Instruments, Elstree, Hertfordshire, UK). Samples were heated from 20 to 275 °C at a rate of 10 °C/min with a nitrogen purge of 40:60 mL/min for the furnace: sample, respectively. TA Universal analysis software (v 4.5A, TA Instruments, Elstree, UK) was used to analyse the data.

2.7. Differential scanning calorimetry (DSC)

Thermal measurement was conducted using a differential scanning calorimeter DSC Q2920 (TA Instruments, Elstree, UK). All samples and raw materials were separately sealed between an aluminum hermetic pan and lid and heated from 10 to 255 °C at a scan rate of 10 °C/min. All measurements were conducted with nitrogen as the purge gas with a flow rate of 60 mL/min. The analysis was performed by TA Universal analysis software (v 4.5A, TA Instruments, Elstree, UK).

2.8. X-ray diffractometry (XRD)

The physical form of the drug and excipients within the laser-cut tablets was assessed using a powder X-ray diffractometer, Miniflex 600 (Rigaku Corporation, Japan). Samples were scanned from 2Theta = 3° to 35° using a 1.25 sec time count and 0.01° step width. The divergence slit was 1 mm, and the scatter slit was 0.6 mm. The filament emission was 10 mA with a scan type coupled with a theta/theta scintillation counter over 60 min. The wavelength was 0.154 nm using Cu^{2+} source and a voltage of 30 kV.

2.9. Drug content of laser-cut tablets

The contents of furosemide were quantified with an Agilent 1260 Series UV-HPLC (Agilent Technologies, Germany) equipped with Kinetex Biphenyl column (50 × 4.6 mm, 2.6 μm particle size) at a temperature of 25 °C. The mobile phase was a 50:50 (v/v) mixture of ammonium acetate buffer (50 mM) and acetonitrile, and the injection volume was 20 μL. The flow rate is maintained at 1 mL/min with a running time of 6 min and a detector wavelength of 254 nm. To determine the level of furosemide impurities following casting and laser cutting processes, an additional HPLC method using Inertsil™ ODS-2 column (250 × 4.6 mm, 5 μm particle size, GL Sciences, Japan) was applied. Potassium dihydrogen phosphate and cetrimide buffer BP: propanol mixture 7:3 (v/v) was used as a mobile phase. The following settings were used: an injection volume of 20 μL, a flow rate of 1 mL/min, a column temperature of 25 °C, a running time of 35 min, and a detector wavelength of 238 nm.

2.10. Characterization of the laser-cut tablets

a. Tablet dimensions and weight

The diameter and thickness of laser-cut tablets (n = 25) were measured using a digital calliper (eSynic, China) with a resolution of 0.01 mm. The tablet thickness measurements were performed by taking the average values of the thickness at a circle inscribes on the four corners of a square and the centre of the tablets. The weight uniformity of laser-cut tablets was assessed by weighing all tablets in the batch. The circularity of the laser-cut tablets was calculated as follows (Mašić et al., 2012):

$$C = 4\pi A/P^2 \quad (1)$$

where P is the total perimeter of the 2D tablet contour and A is the projected area of the 2D tablet contour.

b. Mechanical properties of laser-cut tablets

The mechanical properties of the laser-cutting tablets (n = 6) were assessed by measuring tablet hardness using C50 Tablet Hardness & Compression Testing Machine (Engineering Systems, Nottingham, UK). The friability of laser-cut tablets was assessed by accurately weighing (n = 10) and rotating at 25 rpm for 4 min using Friabilator FT2 (Sotax AG, Switzerland).

c. Surface morphology

The surface morphology of the laser-cut tablets was characterised by Phenom Pro Desktop scanning electron microscope (ThermoFisher Scientific, Paisley, UK) at 10 kV. Tablets were laser cut and attached to a sample holder with double-sided carbon adhesive tape to obtain images of the cross-section and outer surface.

2.11. In vitro disintegration and dissolution

To evaluate the disintegration time of laser-cut tablets, a pharmacopoeia disintegration apparatus (Copley ZT2, Euweka Apparatus GMBH, Heusenstamm, Germany) was used.

Using the USP I dissolution instrument (708-DS dissolution apparatus, Agilent, USA) equipped with inline a UV/VIS spectrophotometer (Cary 60 UV–Vis, Agilent, USA), the *in vitro* furosemide release from laser-cut tablets was determined. Each experiment was conducted in triplicates at 37 ± 0.5 °C and 100 rpm with a rotating basket. The dissolution medium was 900 mL of 0.1 M HCl (pH 1.2) for 2 h at 37 ± 0.5 °C. The samples were measured at 5 min intervals at a 274 nm wavelength and a UV path length of 10 mm. For extended-release tablets (F4-F6), USP pH-change method was applied 2 h at pH 1.2 (750 mL of 0.1 M HCl) followed by 4 h pH 6.8 (the addition of 250 mL of 0.215 M tri-basic sodium phosphate solution to the medium of the gastric phase) and 12 h at pH 7.4.

2.12. Statistical analysis

Standard multiple linear regression using SPSS Software Version 22.0.0.2 (SPSS Inc., Chicago, IL) was conducted to predict the cutting kerf width from laser energy, laser travel speed, and counts. The assumptions of linearity, multicollinearity and homoscedasticity were

assessed and no violation for these were found. One-way ANOVA was employed using SPSS Software (22.0.0.2) to analyse the results. Differences in results less than the probability level ($p < 0.05$) were considered significant.

3. Results and discussion

3.1. Optimisation of polymeric cast for laser-cutting

Laser cutting is theorised to be achieved through fusion (remove), vaporisation, or chemical degradation (flame) (Galtieri et al., 2016; Mushtaq et al., 2020). In this work, the cutting of material was achieved through the melting of thermoplastic polymer by elevating the local temperature at the cutting path above the melting point of the cast (>75 °C). The addition of a light absorber permits the laser to permeate through the polymeric matrix and melt the polymer (Zhang et al., 2021). Initially, different light absorbers were evaluated in drug-polymer casting. The laser-cut section of the polymer casting that contained Gold Sheen was deeper under the same cutting setting (Fig. 3).

In addition, increasing the concentration of Gold Sheen resulted in a deeper cut to the substrate (Fig. 3). Gold Sheen at 1 % was selected due to its ability to achieve a reproducible melting upon the projection of the laser light. The application of laser light has an impact on the surface of the cast substrate. Fig. S2 (Supplementary Data) illustrates the cutting of the edges of the two tablets when the distance between their edges is 0, 1, 2, or 3 mm. While applying a margin of 0 or 1 mm led to the accumulation of molten matter at the edge of the formed tablets, increasing the margin to > 2 mm enabled the completion of the cutting process without altering the tablet surfaces. In many industrial settings, laser cutting is conducted through a predetermined and local melting process, and then the molten material is instantly removed by spraying gas on the substrate (Caiazzo et al., 2005). However, this minimal point-of-care setup did not include a spraying gas mechanism to remove the cut-out structures. Therefore, when the laser is utilised repeatedly to cut the substrate straight onto the substrate, the molten materials are retained at the bottom of the cut cleavage. Without the removal of the molten material, the cut resealed following the cooling of the substrate (data not shown) and the re-solidified molten material impedes the complete cutting of the substrate and the separation of the target shape. To mitigate this, a specially designed template for laser cutting that supports the weight of the laser-cut tablets while allowing the drainage of the molten mater on the laser path (Fig. 2 e1-e3).

The evaluation of the interplay of cutting speed, the number of cutting circles, and the applied laser energy are essential to determine the ideal parameters (Stępak et al., 2016). Fig. 3 illustrated the influences of laser cutting speed, laser energy, and the number of laser cutting counts on cutting depth using SEM imaging. To quantify the different influences, multi-linear regression was conducted, and yielded the following equation to predict the depth of the cut (mm):

$$\text{Depth} = -1535 - 0.376V + 765\ E - 36.3n \quad (2)$$

where V is laser speed (mm/sec), E is laser energy (Watts), and n is the number of laser light applications (rounds).

The depth of the cutting was increased by laser energy and the number of applications and was reduced by the speed of the laser. The multiple regression standardized coefficients revealed that the number of light applications ($\beta = 1.048$, $p < 0.01$) was the most prominent factor

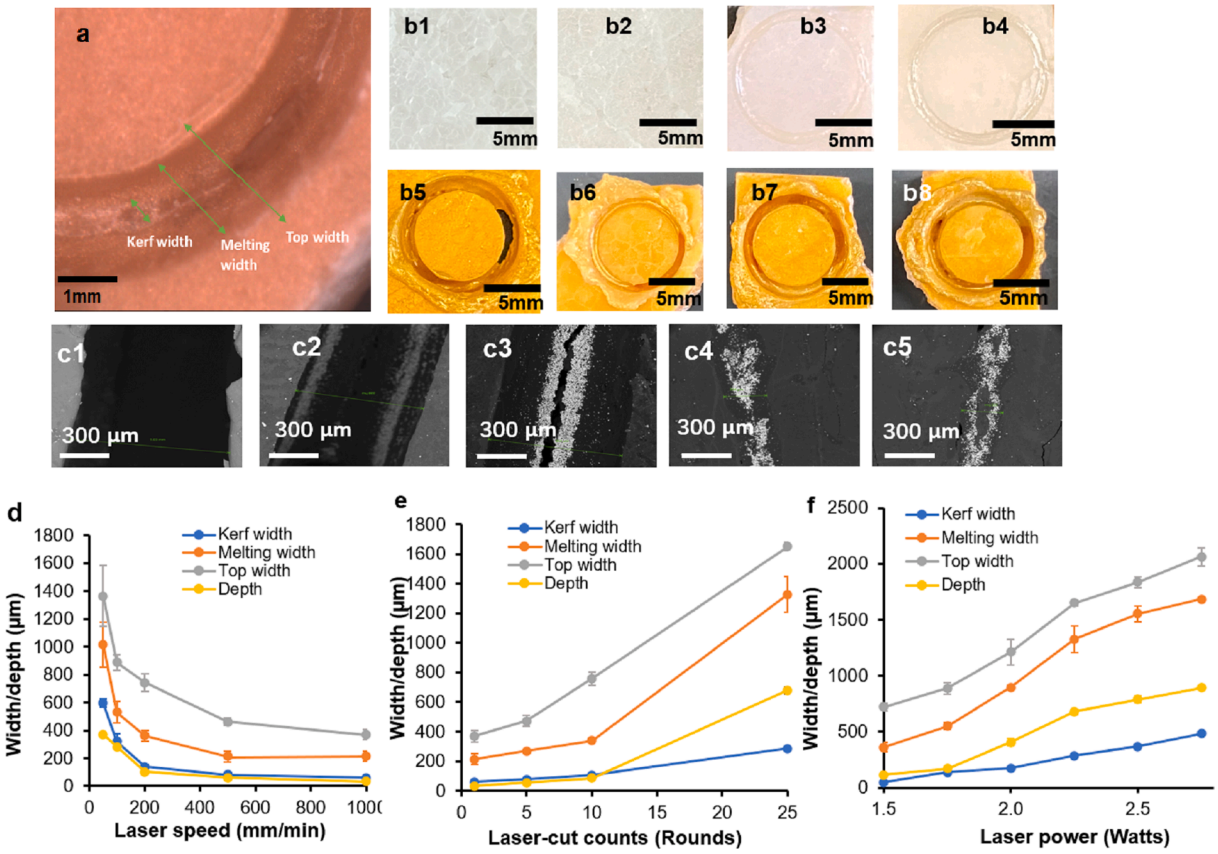

Fig. 3. The laser cutting effect on different drug-free casts: **a1**) polymer casting without an absorbent; **a2**) with 5 % sodium chloride; **a3**) 5 % Blue Shimmer; **a4**) 5 % Silver Sheen; **a5**) 5 %, **a6**) 1 %; **a7**) 2 %, and **a8**) 3 % Gold Sheen. **b**) Light microscope image of a laser cut of the drug-free cast with 2 % gold sheen showing kerf, melting and top widths. SEM images showing the impact of the speed of laser on cutting drug-polymer casts at: **c1**) 100; **c2**) 500; **c3**) 1000; **c4**) 1500; and **c5**) 2000 mm/min. The impact of **d**) laser speed; **e**) laser cutting counts and **f**) laser power on kerf, melting and top widths, and depth. (For interpretation of the references to colour in this figure legend, the reader is referred to the web version of this article.)

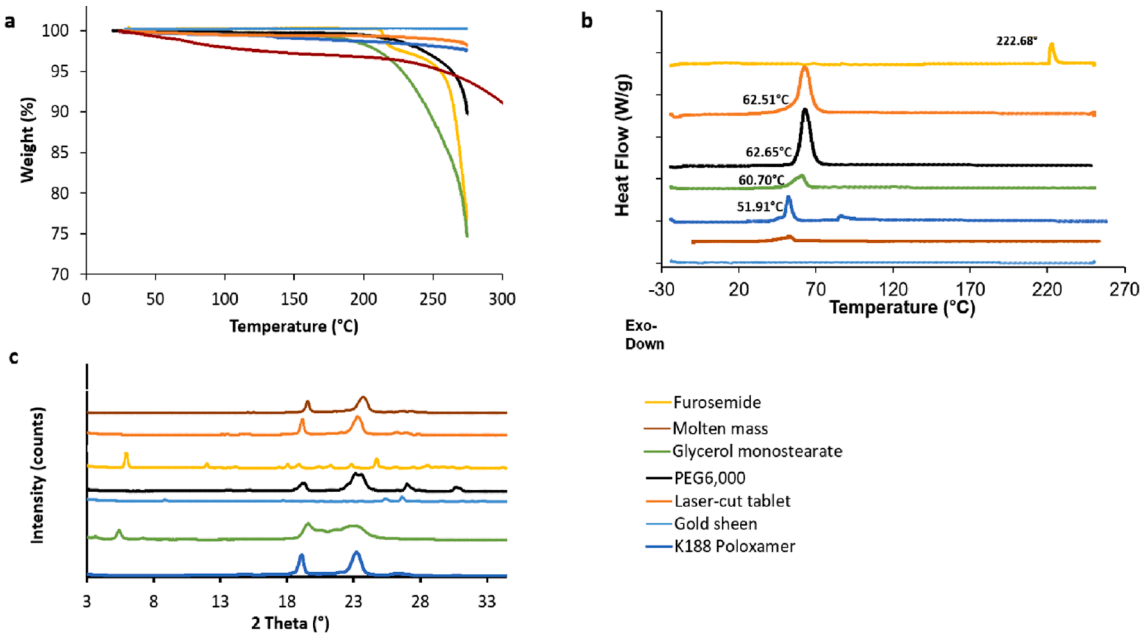

Fig. 4. **a)** TGA thermal degradation profiles, **b)** DSC thermographs, and **c)** XRD intensity patterns of furosemide, other ingredients, and laser-cut tablets.

in predicting the depth of the laser cut, while laser energy ($\beta = 0.406$, $p < 0.01$) and laser speed (standardised coefficient $\beta = -0.376$, $p < 0.001$) had smaller influences. The equation was able to describe 89 % of the total variance ($F(3, 47) = 138.2$, $p < 0.001$).

3.2. Thermal analysis

TGA thermographs were performed to assess the stability of the raw materials at the casting temperature (75 °C). Fig. 4a showed a 0.48 % weight loss of the laser-cut tablet up to 110 °C, which could be attributed due to moisture evaporation. In addition, GMS can be liquefied at a relatively low casting temperature (75 °C) with a melting point of 58–65 °C (Kuźmińska et al., 2021). This facilitates rapid solidification of the casting at room temperature. All raw materials and laser-cut tablets demonstrated stability at 75 °C showing a constant mass, indicating that the manufacture of drug-polymer cast furosemide at this temperature is unlikely to result in significant degradation of furosemide.

DSC thermogram of furosemide exhibited a sharp endothermic peak at 220 °C (Fig. 4b), which corresponds to furosemide melting points and demonstrates its crystalline nature (Jassimp, 2017). The characteristic furosemide peak was not observed in the thermogram of the laser-cut tablet nor in the molten mass, confirming that furosemide was present in the amorphous state within the polymer substrate (Nkansah et al., 2013). It is also possible that due to the melting of PEG 6000 during the thermal scan, the molten polymer has dissolved drug crystals before they are able to reach their melting point (Newa et al., 2008). DSC thermographs of the laser-cut tablets also showed an endotherm event at ~ 62 °C (Fig. 4b), which could be attributed to the suppressed melting of PEG 6000, indicating the presence of a portion of PEG 6000 and GMS in a crystalline form. Therefore, the laser beam that can introduce a localised increase in temperature > 70 °C was deemed necessary to liquidate GMS and PEG 6000 crystals and allow efficacious laser-cutting of the formulation.

The XRD pattern of the laser-cut tablets revealed characteristic furosemide diffraction peaks at $2(\theta) = 5.94°$, 11.23° and 24.72° (Fig. 4c). At $2(\theta) = 19.57°$, a subtle peak corresponding to GMS, can be observed (Fig. 4c). This indicated the presence of GMS crystals in the polymeric matrix. The absence of an intensity peak at $2(\theta) = 5.94°$ confirms the findings of the thermal analysis that no crystalline form of furosemide could be detected in the laser-cut tablets and the molten mass.

3.3. Impurity analysis using HPLC

Furosemide is labile to thermal (Jassimp, 2017) and light degradation (Asker and Ferdous, 1996). The relative laser energy input to laser cut by melting thermoplastic polymeric substrate might have an impact on the integrity of the model molecule. A summary of HPLC analysis of furosemide impurities is presented in Fig. 5 (Supplementary Data, Table S2). Furosemide concentration exceeds 99 % in both a non-laser-cut corner of the drug-polymer casting as well as the laser-cut tablets. It has been demonstrated that neither the substrate manufacturing process nor the laser cutting process resulted in significant degradation of furosemide ($p > 0.05$).

This could be attributed to the use of a low-energy laser and the brief light exposure time during laser cutting (<1 min). In addition, most of the laser exposure is directed to the heat-affected zone (HAZ), which resulted in a significant drop in furosemide contents (97.41 %) and a rise of impurity C (2.39 %) in the discharged molten mass (Fig. 5).

3.4. Characteristics of laser-cut tablets

Fig. 6a-b illustrates that laser cutting can be used to engrave a logo. This feature can be used to specify the patient's details on a patient-specific dosage form. The laser-cut tablets have smooth surfaces with a glossy look. To demonstrate the potential of the method to produce personalised tablets, four batches of laser-cut tablets (n = 25) of different diameters were manufactured. Table 1 shows the dimensions, and compendial characteristics of laser-cut tablets with furosemide doses of 5, 7.5, 10, or 15 mg. While the thickness of each tablet was kept at 3 mm, the furosemide dose was controlled by digitally altering the diameter of the design (Table 1). The relationship between the tablet weight and volume was confirmed to be directly proportional (Fig. 6d). The deviation from the linear relationship could be attributed to variations in the thickness of the cast. In addition, the cutting kerf in the used process was measured to be in the range of 1.45–1.59 mm. The variation in dimensions was minimal with a relative standard deviation range (SD %) of 1.43 %-1.95 % (Table 2), this partially contributed to a variation in

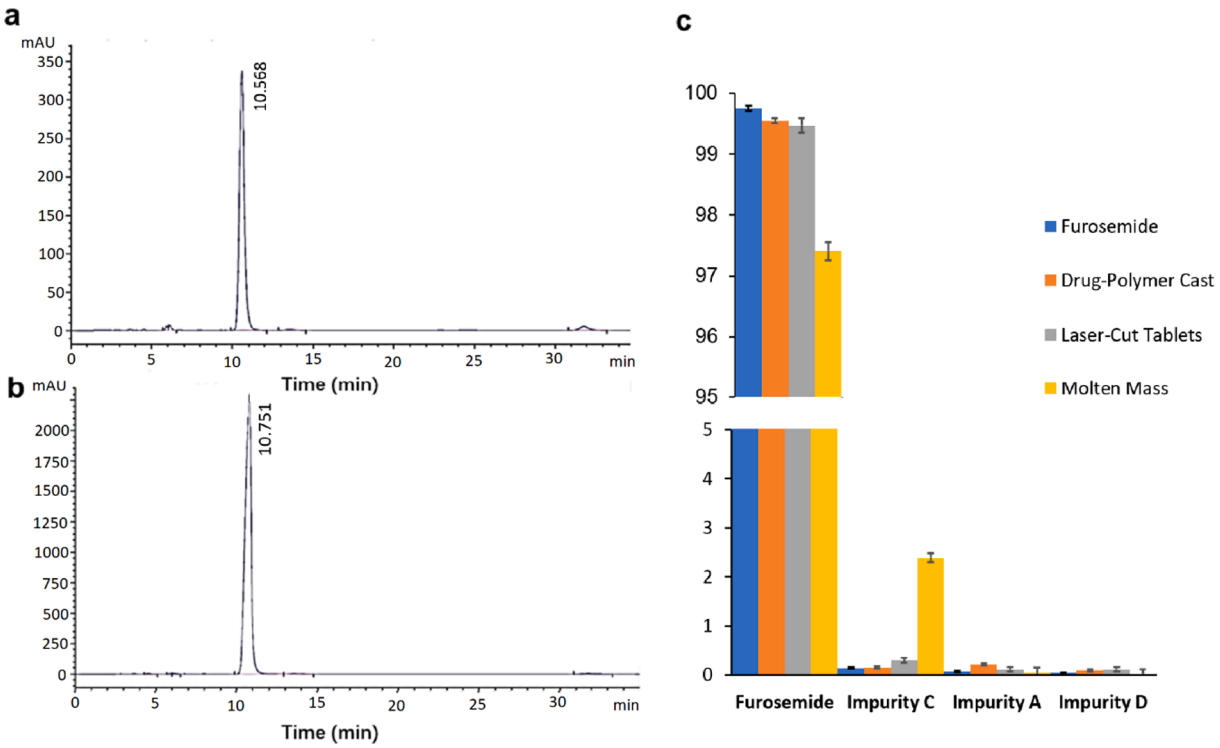

Fig. 5. Chromatograms of **a**) laser-cut tablet pure furosemide, **b**) pure furosemide, and **c**) the percentage of purity of furosemide, drug-polymer casts, and laser-cut tablets.

the laser-cut tablet weights with an SD% range of 2.7 %-4.66 %. The circularity values of the laser-cut tablets were in the range of 0.996–1.0004, indicating that this approach is capable of producing tablets of high roundness (Mašić et al., 2012). While the surface cut for each tablet is identical, a slight variation in the thickness of the cast would result in deviation from the theoretical weight. In addition, the laser-cut tablets demonstrated a side surface that deviates from a vertical straight cutline. This could be attributed to the mechanism of kerf formation. When the surface temperature reaches > 60 °C, the polymer material starts to melt, creating a melt pool in the material removal zone, which will expand until it penetrates the full thickness of the workpiece and forms a complete kerf. When the cut thickness is relatively thick, heat transfer in the cutting direction can expand from the bottom diagonal surface in the horizontal direction, thus allowing more material to be melted in the middle of the laser cross-section (Choi et al., 2022).

The content uniformity test showed that all batches of tablets met British Pharmacopoeia (BP) standards. These laser-cut tablets have a pharmaceutically acceptable degree of fragility (<1%), hence, demonstrating the durability of laser-cut tablets to withstand the production, shipping, and administration processes (Wasilewska and Winnicka, 2019). The process also demonstrated a high degree of repeatability, as evidenced by minimal variations in tablet weight and drug content. Therefore, this highlights the potential of this laser-cutting approach as an alternative small-batch production approach.

The disintegration times of laser-cut tablets prepared by casting and laser cutting are reported in Table 1. The relatively short disintegration period of laser-cut tablets can be attributed to the hydrophilic nature of PEG 6000, which promotes the passage of water into the tablet core and shortens the disintegration time (Bai et al., 2021). Fig. 6e demonstrated that the developed drug formulation has a rapid-release profile. The tablets from different sizes (F3) released more than 75 % of the drugs within 45 min, meeting the British Pharmacopoeia (BP) criteria for immediate-release dosage forms. The fast dissolution of furosemide could be attributed to the presence of furosemide in amorphous form, where little energy is needed to break the crystal lattice during the dissolution process (Dong et al., 2020). In addition, the solubilising effect of PEG 6000 for poorly soluble drugs (Biswal et al., 2008; Liw et al., 2022) has been extensively reported. Such an effect on drug release was proposed to be carrier-mediated (Saers and Craig, 1992).

3.5. *Furosemide release from laser-cut tablets*

The potential of this approach to yield extended drug release was explored by increasing the ratio of lipophilic glyceride (GMS). Fig. 6f indicated that higher GMS contents yielded extended drug release in the intestinal phase (F4-F6). GMS was reported to inhibit drug release from alginate-based films (Khoder et al., 2020).

Upon pH change, drug release was significantly accelerated. This could be attributed to the higher solubility of furosemide in the intestinal medium (Devarakonda et al., 2007; Rowbotham et al., 1976). Ritger-Peppas model demonstrated an exponent n > 1, indicating a super Case II transport (Mohanta and Thirugnanam, 2023; Ye et al., 2023). In addition, SEM images of the laser-cut tablets following dissolution (Fig. 7d1-d6), illustrated the formation of pores within the matrix structure due to the erosion of the soluble components, leaving an insoluble skeleton.

Fig. 1 provides a comparison of laser cutting compared to other tablet manufacturing technologies. Compared to standard powder compression, laser cutting does not involve numerous processing steps, which are very operator-dependent (Bowles et al., 2018; Sandler et al., 2011b) The primary advantages of laser cutting are its simple and convenient operation, short production time, and ability to make one tablet in a relatively short period (<1min), while the printing time using 3D printing was 4 min per tablet (Clark et al., 2017). One important advantage of the laser cutting approach is avoiding the modification of the structure of the matrix during the production process. This is significantly different from additive (3DP) and formative (powder

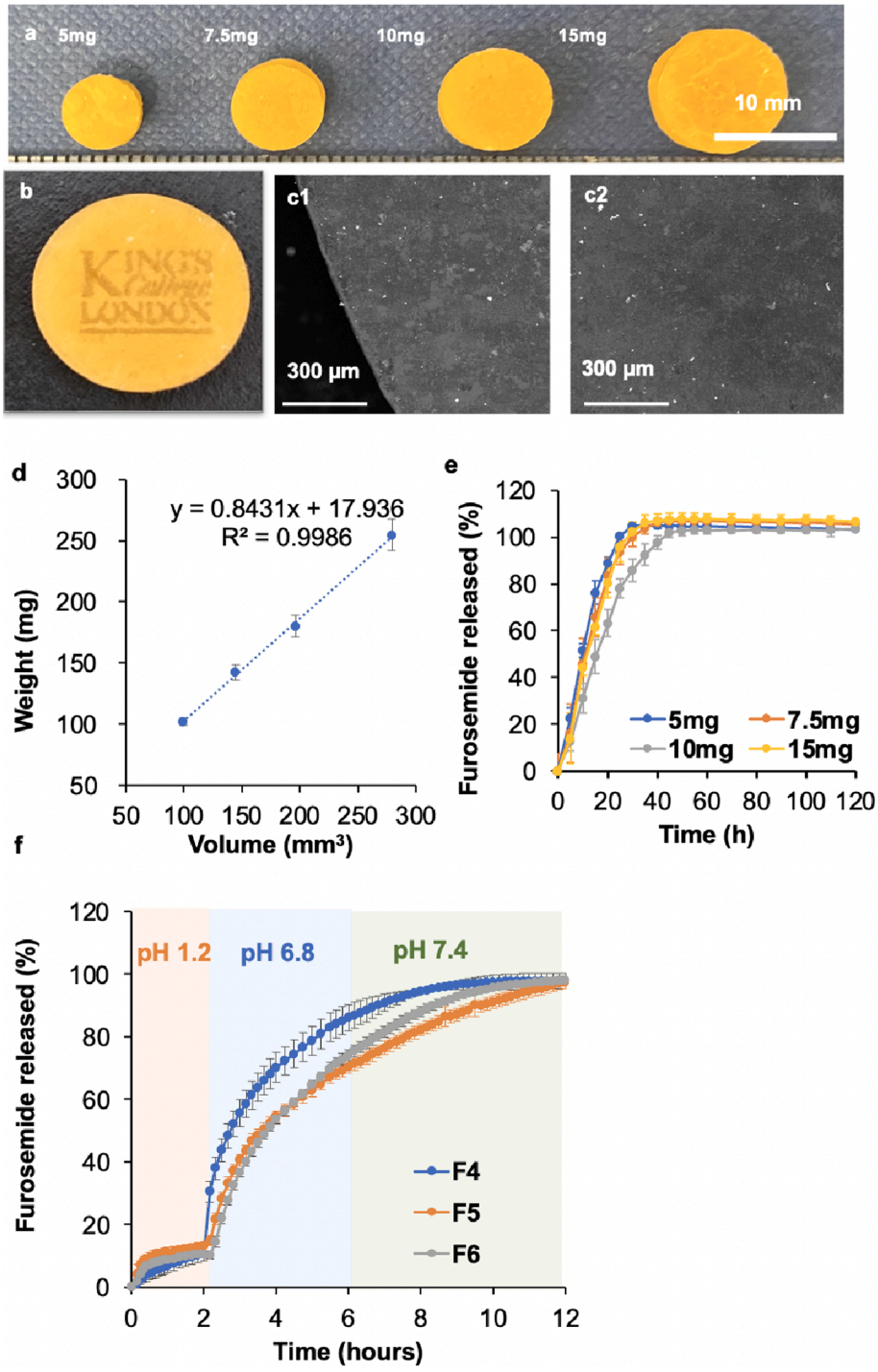

Fig. 6. Laser cutting tablets with target doses: **a**) Images of the tablet containing 5, 7.5, 10, or 15 mg of furosemide (F3); **b**) laser-cut tablets personalised with engraved university logo; SEM image of **c1**) cross-section and **c2**) surface of immediate release laser-cut tablet (**d**) The volume-mass relationship of tablets with target doses of 5, 7.5, 10 and 15 mg. In vitro release of furosemide from **e**) immediate release (F3) and **f**) extended-release tablets (F4-F6) laser-cut tablets (F3) of different sizes using USPII dissolution test, n = 3, ±SD.

Table 1
Measured weights, dimensions, volumes, surface area, surface/mass and surface/volume ratios, drug content, disintegrate time, tensile strength, and friability of laser-cutting furosemide tablets (n = 20).

Furosemide target dose (mg)	Tablet weight (mg)	Diameter (mm) ±SD (SD%)	Height (mm)	Volume (mm^3)	Surface area (mm^2)	Surface/ mass (mm^2/mg)	Surface/ volume (mm^{-1})	Drug content (mg)	Disintegration time (min)	Tensile strength (MPa)	Friability (%)
5	99.53 ± 2.74	6.15 ± 0.12 (1.95 %)	3.44 ± 0.12	101.74 ± 3.47	125.44 ± 2.67	1.26 ± 0.02	1.23 ± 0.03	4.98 ± 0.14	11.92 ± 1.90	0.83 ± 0.03	0.16
7.5	144.50 ± 6.49	7.26 ± 0.14 (1.93 %)	3.43 ± 0.13	142.00 ± 7.20	161.05 ± 5.01	1.12 ± 0.02	1.14 ± 0.03	7.22 ± 0.32	11.87 ± 0.71	0.79 ± 0.04	0.17
10	196.09 ± 9.13	8.41 ± 0.12 (1.43 %)	3.24 ± 0.18	179.90 ± 8.34	196.79 ± 3.87	1.01 ± 0.03	1.10 ± 0.03	9.80 ± 0.46	12.10 ± 0.98	0.86 ± 0.08	0.13
15	279.16 ± 12.93	9.95 ± 0.16 (1.61 %)	3.26 ± 0.13	254.56 ± 12.21	258.2 ± 6.43	0.93 ± 0.03	1.12 ± 0.03	13.95 ± 0.65	9.63 ± 0.87	0.77 ± 0.07	0.34

Table 2
Summary of the diameter of laser path, kerf width, circularity, and a breakdown of workpiece usage for laser-cut furosemide tablets.

Furosemide target dose (mg)	Diameter of the laser path(mm)	Kerf width(mm)	Circularity	Tablets area (%)	Laser-affected areas (%)	Unused area (%)
5	7.6	1.45	1.004	12.5 %	6.60 %	81 %
7.5	8.8	1.54	0.998	17.5 %	8.19 %	74 %
10	10	1.59	0.998	23.4 %	9.69 %	67 %
15	11.5	1.55	0.996	32.8 %	11.01 %	56 %

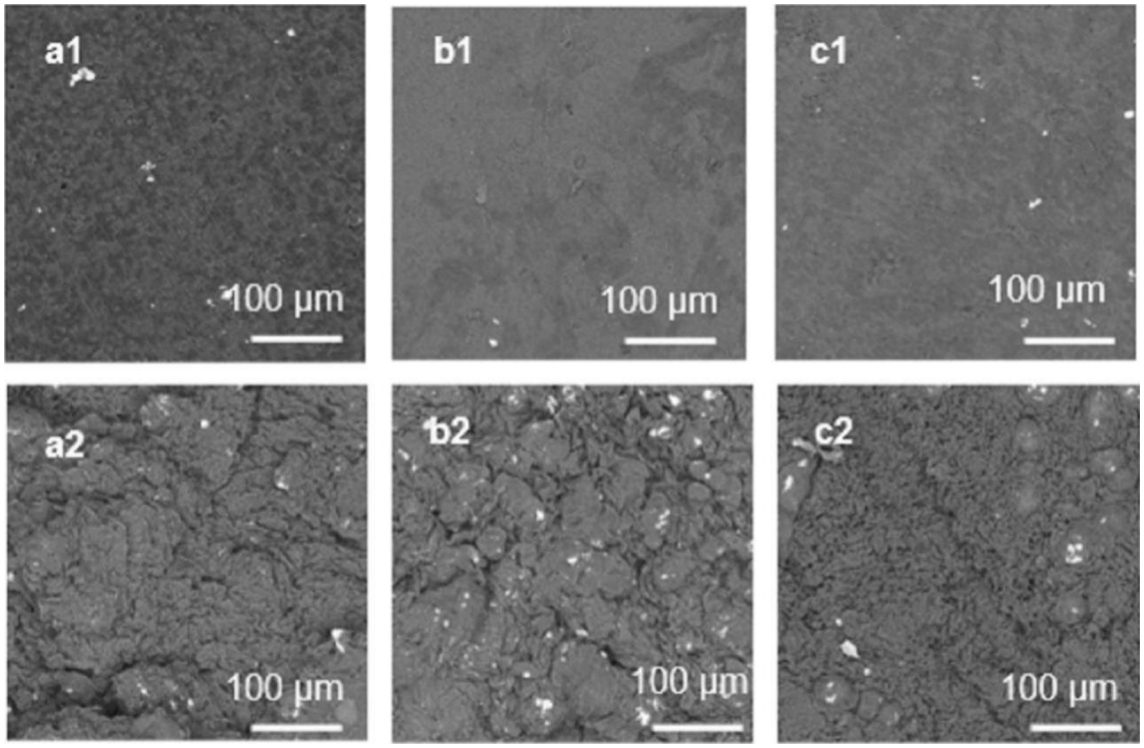

Fig. 7. SEM image of extended-release laser cut tablets (F4- F6) before (**d1-d3**) and after (**d4-d6**) dissolution.

compression) manufacturing, where the tablet formation process could alter the final tablet structure e.g., the physical form of the drug or matrix density of the tablet. Hence, this approach is less likely to modify critical quality attributes (CQAs) such as release patterns or drug contents (Goodwin et al., 2018; Markl et al., 2020). This is a significant advantage that can simplify quality control (QC) and a real-time release of tablet batches produced in a point-of-care manufacturing scenario.

The presented setup used 12.5 % to 32.8 % of the workpiece to produce tablets with a wastage of 6.6 %-11 % in a form of a molten mass, leaving > 55 % of the workpiece unused (Table 2). Several approaches could be applied to lower waste. For instance, minimising the margins between tablets through narrowing the distance between the tablets or the modification of tablet geometry e.g., replacing the round shape with a hexagon. In addition, narrowing the thickness of the workpiece could shorten the time of the kerf formation and minimize laser exposure, hence improving process efficiency and decreasing the waste of material through degradation (Choi et al., 2022). To improve process efficiency, further research is needed to determine whether the marginal materials can be recycled.

While this manufacturing approach has been exemplified by producing small batches of tablets, it could be potentially applied to other drug delivery systems such as implants and wound dressings (Teoh et al., 2022).

4. Conclusion

To the best of the authors' knowledge, this research is the first investigation into the application of laser cutting technology for on-demand tablet manufacturing. The study focused on optimising the parameters of laser cutting to achieve a precise cut of a specially formulated drug-polymer cast with minimal degradation of the active ingredient. By adjusting the digital design, the novel laser-cutting procedure enabled the production of bespoke furosemide tablets with a specific morphology, surface engraving and size. The laser-cutting process induced minimal changes to the matrix structure, potentially simplifying the quality control (QC) steps required for batch release. Liquid chromatography confirmed that furosemide degradation and impurity formation following laser cutting were minimal, and the laser-cutting approach demonstrated its consistency with the manufacturing of a batch of tablets of consistent quality. The release from the laser cut matrix appeared to be largely governed by an erosion mechanism with the potential of immediate fast and extended-release profiles. This innovative technological approach offers a promising alternative to conventional methods for point-of-care manufacturing.

CRediT authorship contribution statement

Yujing Liu: Investigation, Methodology, Writing – original draft. **Anna M Leonova:** Investigation. **Paul G. Royall:** Methodology, Writing – review & editing. **Bambang V.E.B. Abdillah Akbar:** Investigation. **Zhengge Cao:** Investigation. **Stuart A. Jones:** Methodology, Writing – review & editing. **Abdullah Isreb:** . **Daniel B. Hawcutt:** Writing – review & editing. **Mohamed A. Alhnan:** Conceptualization, Supervision, Software, Writing – review & editing, Project administration.

Declaration of Competing Interest

The authors declare that they have no known competing financial interests or personal relationships that could have appeared to influence the work reported in this paper.

Data availability

The authors are unable or have chosen not to specify which data has been used.

Appendix A. Supplementary data

Supplementary data to this article can be found online at https://doi.org/10.1016/j.ijpharm.2023.123518.

References

Albarahmieh, E., AbuAmmouneh, L., Kaddoura, Z., AbuHantash, F., Alkhalidi, B.A., Al-Halhouli, A., 2019. Fabrication of dissolvable microneedle patches using an innovative laser-cut mould design to shortlist potentially transungual delivery systems: In vitro evaluation. AAPS PharmSciTech 20, 215. https://doi.org/10.1208/s12249-019-1429-5.

Asker, A.F., Ferdous, A.J., 1996. Photodegradation of Furosemide Solutions. PDA J. Pharm. Sci. Technol. 50.

Awad, A., Yao, A., Trenfield, S.J., Goyanes, A., Gaisford, S., Basit, A.W., 2020. 3D Printed Tablets (Printlets) with Braille and Moon Patterns for Visually Impaired Patients. Pharmaceutics 12, 172. https://doi.org/10.3390/pharmaceutics12020172.

Bai, Y., Wang, D., Zhang, Z., Pan, J., Cui, Z., Yu, D.G., Annie Bligh, S.W., 2021. Testing of fast dissolution of ibuprofen from its electrospun hydrophilic polymer nanocomposites. Polym. Test. 93, 106872 https://doi.org/10.1016/J.POLYMERTESTING.2020.106872.

Biswal, S., Sahoo, J., Murthy, P.N., Giradkar, R.P., Avari, J.G., 2008. Enhancement of Dissolution Rate of Gliclazide Using Solid Dispersions with Polyethylene Glycol 6000. AAPS PharmSciTech 9, 563–570. https://doi.org/10.1208/s12249-008-9079-z.

Bowles, B.J., Dziemidowicz, K., Lopez, F.L., Orlu, M., Tuleu, C., Edwards, A.J., Ernest, T. B., 2018. Co-Processed Excipients for Dispersible Tablets-Part 1: Manufacturability. AAPS PharmSciTech 19, 2598–2609. https://doi.org/10.1208/s12249-018-1090-4.

Brion, L.P., Primhak, R.A., Yong, W., 2001. Aerosolized diuretics for preterm infants with (or developing) chronic lung disease. Cochrane Database Syst. Rev. https://doi.org/10.1002/14651858.CD001694.

Caiazzo, F., Curcio, F., Daurelio, G., Minutolo, F.M.C., 2005. Laser cutting of different polymeric plastics (PE, PP and PC) by a CO2 laser beam. J. Mater. Process. Technol. 159, 279–285. https://doi.org/10.1016/j.jmatprotec.2004.02.019.

Cairone, F., Gallo Afflitto, F., Stella, G., Cicala, G., Ashour, M., Kersaudy-Kerhoas, M., Bucolo, M., 2022. Micro-Optical Waveguides Realization by Low-Cost Technologies. Micro 2, 123–136. https://doi.org/10.3390/micro2010008.

Choi, J., Kim, R., Song, D., Cho, D.-W., Suh, J., Kim, S., Ahn, S.-H., 2022. Analysis of Laser Cutting Process for Different Diagonal Material Shapes. Processes 10, 2743. https://doi.org/10.3390/pr10122743.

Choonara, Y.E., Du Toit, L.C., Kumar, P., Kondiah, P.P.D., Pillay, V., 2016. 3D-printing and the effect on medical costs: a new era? Expert Rev. Pharmacoecon. Outcomes Res. 16, 23–32. https://doi.org/10.1586/14737167.2016.1138860.

Clark, E.A., Alexander, M.R., Irvine, D.J., Roberts, C.J., Wallace, M.J., Sharpe, S., Yoo, J., Hague, R.J.M., Tuck, C.J., Wildman, R.D., 2017. 3D printing of tablets using inkjet with UV photoinitiation. Int. J. Pharm. 529, 523–530. https://doi.org/10.1016/J.IJPHARM.2017.06.085.

Crișan, A.G., Iurian, S., Porfire, A., Rus, L.M., Bogdan, C., Casian, T., Lucacel, R.C., Turza, A., Porav, S., Tomuță, I., 2022. QbD guided development of immediate release FDM-3D printed tablets with customizable API doses. Int. J. Pharm. 613 https://doi.org/10.1016/j.ijpharm.2021.121411.

Devarakonda, B., Otto, D., Judefeind, A., Hill, R., Devilliers, M., 2007. Effect of pH on the solubility and release of furosemide from polyamidoamine (PAMAM) dendrimer complexes. Int. J. Pharm. 345, 142–153. https://doi.org/10.1016/j.ijpharm.2007.05.039.

Dong, C.L., Zheng, S.D., Liu, Y.Y., Cui, W.Q., Hao, M.Q., God'spower, B.O., Chen, X.Y., Li, Y.H., 2020. Albendazole solid dispersions prepared using PEG6000 and Poloxamer188: formulation, characterization and in vivo evaluation. Pharm. Dev. Technol. 25, 1043–1052. https://doi.org/10.1080/10837450.2020.1783553/SUPPL_FILE/IPHD_A_1783553_SM9490.DOCX.

Elsheikh, A.H., Deng, W., Showaib, E.A., 2020. Improving laser cutting quality of polymethylmethacrylate sheet: Experimental investigation and optimization. J. Mater. Res. Technol. 9 https://doi.org/10.1016/j.jmrt.2019.11.059.

Galtieri, G., Visco, A., Nocita, D., Torrisi, L., Ceccio, G., Scolaro, C., 2016. Polyethylene laser welding based on optical absorption variations. J. Instrum. 11, C04013–C. https://doi.org/10.1088/1748-0221/11/04/C04013.

Goodwin, D.J., van den Ban, S., Denham, M., Barylski, I., 2018. Real time release testing of tablet content and content uniformity. Int. J. Pharm. 537 https://doi.org/10.1016/j.ijpharm.2017.12.011.

Guo, X., Deng, M., Hu, Y., Wang, Y., Ye, T., 2021. Morphology, mechanism and kerf variation during CO_2 laser cutting pine wood. J. Manuf. Process. 68, 13–22. https://doi.org/10.1016/j.jmapro.2021.05.036.

Heberle, J., Häfner, T., Schmidt, M., 2018. Efficient and damage-free ultrashort pulsed laser cutting of polymer intraocular lens implants. CIRP Ann. 67 https://doi.org/10.1016/j.cirp.2018.04.095.

Jassimp, Z.E., 2017. Formulation and evaluation of furosemide liquisolid compact. Int. J. Appl. Pharm. 9, 39–48. https://doi.org/10.22159/IJAP.2017V9I6.21458.

Kaba, K., Purnell, B., Liu, Y., Royall, P.G., Alhnan, M.A., 2023. Computer numerical control (CNC) carving as an on-demand point-of-care manufacturing of solid dosage form: A digital alternative method for 3D printing. Int. J. Pharm. 645, 123390 https://doi.org/10.1016/j.ijpharm.2023.123390.

Khaled, S.A., Burley, J.C., Alexander, M.R., Roberts, C.J., 2014. Desktop 3D printing of controlled release pharmaceutical bilayer tablets. Int. J. Pharm. 461 https://doi.org/10.1016/j.ijpharm.2013.11.021.

Khoder, M., Schropp, V., Zeitler, S., Pereira, B., Habashy, R., Royall, P.G., Wang, J.T.W., Alhnan, M.A., 2020. A novel natural GRAS-grade enteric coating for pharmaceutical and nutraceutical products. Int. J. Pharm. 584 https://doi.org/10.1016/j.ijpharm.2020.119392.

Kozakiewicz-Latała, M., Nartowski, K.P., Dominik, A., Malec, K., Gołkowska, A.M., Złocińska, A., Rusińska, M., Szymczyk-Ziółkowska, P., Ziółkowski, G., Górniak, A., Karolewicz, B., 2022. Binder jetting 3D printing of challenging medicines: From low dose tablets to hydrophobic molecules. Eur. J. Pharm. Biopharm. 170 https://doi.org/10.1016/j.ejpb.2021.11.001.

Krueger, L., Miles, J.A., Popat, A., 2022. 3D printing hybrid materials using fused deposition modelling for solid oral dosage forms. J. Control. Release 351, 444–455. https://doi.org/10.1016/j.jconrel.2022.09.032.

Kuźmińska, M., Pereira, B.C., Habashy, R., Peak, M., Isreb, M., Gough, T.D., Isreb, A., Alhnan, M.A., 2021. Solvent-free temperature-facilitated direct extrusion 3D printing for pharmaceuticals. Int. J. Pharm. 598 https://doi.org/10.1016/J.IJPHARM.2021.120305.

Kyobula, M., Adedeji, A., Alexander, M.R., Saleh, E., Wildman, R., Ashcroft, I., Gellert, P. R., Roberts, C.J., 2017. 3D inkjet printing of tablets exploiting bespoke complex geometries for controlled and tuneable drug release. J. Control. Release 261. https://doi.org/10.1016/j.jconrel.2017.06.025.

Littler, T.B., Morrow, D.J., 1999. Wavelets for the analysis and compression of power system disturbances. IEEE Trans. Power Delivery 14, 358–364. https://doi.org/10.1109/61.754074.

Liw, J.J., Teoh, X.-Y., Teoh, A.X.Y., Chan, S.-Y., 2022. The Effect of Carrier-Drug Ratios on Dissolution Performances of Poorly Soluble Drug in Crystalline Solid Dispersion System. J. Pharm. Sci. 111, 95–101. https://doi.org/10.1016/j.xphs.2021.06.026.

Markl, D., Warman, M., Dumarey, M., Bergman, E.L., Folestad, S., Shi, Z., Manley, L.F., Goodwin, D.J., Zeitler, J.A., 2020. Review of real-time release testing of pharmaceutical tablets: State-of-the art, challenges and future perspective. Int. J. Pharm. https://doi.org/10.1016/j.ijpharm.2020.119353.

Mašić, I., Ilić, I., Dreu, R., Ibrić, S., Parojčić, J., Đurić, Z., 2012. An investigation into the effect of formulation variables and process parameters on characteristics of granules obtained by in situ fluidized hot melt granulation. Int. J. Pharm. 423, 202–212. https://doi.org/10.1016/j.ijpharm.2011.12.013.

Melnikova, R., Ehrmann, A., Finsterbusch, K., 2014. 3D printing of textile-based structures by Fused Deposition Modelling (FDM) with different polymer materials. IOP Conf Ser Mater Sci Eng 62, 012018. https://doi.org/10.1088/1757-899X/62/1/012018.

Mohanta, M., Thirugnanam, A., 2023. Development of Multifunctional Commercial Pure Titanium-Polyethylene Glycol Drug-Eluting Substrates with Enhanced Optical and Antithrombotic Properties. Cardiovasc. Eng. Technol. 14, 37–51. https://doi.org/10.1007/s13239-022-00637-z.

Moradi, M., Moghadam, M.K., Shamsborhan, M., Bodaghi, M., Falavandi, H., 2020. Post-processing of FDM 3d-printed polylactic acid parts by laser beam cutting. Polymers (basel) 12. https://doi.org/10.3390/polym12030550.

Moradi, M., Moghadam, M.K., Shamsborhan, M., Beiranvand, Z.M., Rasouli, A., Vahdati, M., Bakhtiari, A., Bodaghi, M., 2021. Simulation, statistical modeling, and optimization of CO2 laser cutting process of polycarbonate sheets. Optik (stuttg) 225. https://doi.org/10.1016/j.ijleo.2020.164932.

Mushtaq, R.T., Wang, Y., Rehman, M., Khan, A.M., Mia, M., 2020. State-Of-The-Art and Trends in CO2 Laser Cutting of Polymeric Materials—A Review. Materials 13, 3839. https://doi.org/10.3390/ma13173839.

Newa, M., Bhandari, K.H., Kim, J.-A., Yoo, B.-K., Choi, H.-G., Yong, C.-S., Woo, J.-S., Lyoo, W.-S., 2008. Preparation and Evaluation of Fast Dissolving Ibuprofen-Polyethylene Glycol 6000 Solid Dispersions. Drug Deliv. 15, 355–364. https://doi.org/10.1080/10717540801952431.

Nkansah, P., Antipas, A., Lu, Y., Varma, M., Rotter, C., Rago, B., El-Kattan, A., Taylor, G., Rubio, M., Litchfield, J., 2013. Development and evaluation of novel solid nanodispersion system for oral delivery of poorly water-soluble drugs. J. Control. Release 169, 150–161. https://doi.org/10.1016/j.jconrel.2013.03.032.

Öblom, H., Sjöholm, E., Rautamo, M., Sandler, N., 2019. Towards Printed Pediatric Medicines in Hospital Pharmacies: Comparison of 2D and 3D-Printed Orodispersible Warfarin Films with Conventional Oral Powders in Unit Dose Sachets. Pharmaceutics 11. https://doi.org/10.3390/PHARMACEUTICS11070334.

Peng, S., Li, T., Wang, X., Dong, M., Liu, Z., Shi, J., Zhang, H., 2017. Toward a Sustainable Impeller Production: Environmental Impact Comparison of Different Impeller Manufacturing Methods. J. Ind. Ecol. 21 https://doi.org/10.1111/jiec.12628.

Prandota, J., 2001. Clinical pharmacology of furosemide in children: A supplement. Am. J. Ther. 8, 275–289. https://doi.org/10.1097/00045391-200107000-00010.

Rowbotham, P.C., Stanford, J.B., Sugden, J.K., 1976. Some aspects of the photochemical degradation of frusemide. Pharm. Acta Helv. 51.

Sadia, M., Arafat, B., Ahmed, W., Forbes, R.T., Alhnan, M.A., 2018. Channelled tablets: An innovative approach to accelerating drug release from 3D printed tablets. J. Control. Release 269, 355–363. https://doi.org/10.1016/j.jconrel.2017.11.022.

Saers, E.S., Craig, D.Q.M., 1992. An investigation into the mechanisms of dissolution of alkyl p-aminobenzoates from polyethylene glycol solid dispersions. Int. J. Pharm. 83, 211–219. https://doi.org/10.1016/0378-5173(82)90024-2.

Sandler, N., Määttänen, A., Ihalainen, P., Kronberg, L., Meierjohann, A., Viitala, T., Peltonen, J., 2011. Inkjet printing of drug substances and use of porous substrates-towards individualized dosing. J. Pharm. Sci. 100, 3386–3395. https://doi.org/10.1002/JPS.22526.

Seo, Y., Lee, D., Pyo, S., 2020. High-Power Fiber Laser Cutting for 50-mm-Thick Cement-Based Materials. Materials 13 (5), 1113. https://doi.org/10.3390/ma13051113.

Stępak, B., Antończak, A.J., Abramski, K.M., 2016. Optimization of femtosecond laser cutting of a biodegradable polymer for medical devices manufacturing. Photonics Lett Pol 8, 116–118. https://doi.org/10.4302/PLP.2016.4.09.

Teoh, J.H., Tay, S.M., Fuh, J., Wang, C.-H., 2022. Fabricating scalable, personalized wound dressings with customizable drug loadings via 3D printing. J. Control. Release 341, 80–94. https://doi.org/10.1016/j.jconrel.2021.11.017.

Trenfield, S.J., Awad, A., Goyanes, A., Gaisford, S., Basit, A.W., 2018. 3D Printing Pharmaceuticals: Drug Development to Frontline Care. Trends Pharmacol. Sci. 39, 440–451. https://doi.org/10.1016/J.TIPS.2018.02.006.

Wasilewska, K., Winnicka, K., 2019. How to assess orodispersible film quality? A review of applied methods and their modifications. Acta Pharm. 69, 155–176. https://doi.org/10.2478/ACPH-2019-0018.

Yang, T.L., Stogiannari, M., Janeczko, S., Khoshan, M., Lin, Y., Isreb, A., Habashy, R., Giebułtowicz, J., Peak, M., Alhnan, M.A., 2023a. Towards point-of-care manufacturing and analysis of immediate-release 3D printed hydrocortisone tablets for the treatment of congenital adrenal hyperplasia. Int J Pharm 642. https://doi.org/10.1016/j.ijpharm.2023.123072.

Yang, T.L., Szewc, J., Zhong, L., Leonova, A., Giebułtowicz, J., Habashy, R., Isreb, A., Alhnan, M.A., 2023b. The use of near-infrared as process analytical technology (PAT) during 3D printing tablets at the point-of-care. Int J Pharm 642. https://doi.org/10.1016/j.ijpharm.2023.123073.

Ye, J., Liu, L., Lan, W., Xiong, J., 2023. Targeted release of soybean peptide from CMC/PVA hydrogels in simulated intestinal fluid and their pharmacokinetics. Carbohydr. Polym. 310, 120713 https://doi.org/10.1016/j.carbpol.2023.120713.

Zhang, Y., Zhang, J., Thakkar, R., Pillai, A.R., Wang, J., Lu, A., Maniruzzaman, M., 2021. Functions of Magnetic Nanoparticles in Selective Laser Sintering (SLS) 3D Printing of Pharmaceutical Dosage Forms. https://doi.org/10.26434/CHEMRXIV.13925177.V1.